JOURNAL OF CATALYSIS **178,** 66–75 (1998)
ARTICLE NO. CA982122

The Effect of Potassium and Tin on the Hydrogenation of Ethylene and Dehydrogenation of Cyclohexane over Pt(111)

Yong-Ki Park,[1] Fabio H. Ribeiro,[2] and Gabor A. Somorjai

Materials Sciences Division, Ernest Orlando Lawrence Berkeley National Laboratory, Berkeley, California, 94720 and Department of Chemistry, University of California, Berkeley, California 94720

Received October 16, 1997; revised April 8, 1998; accepted April 28, 1998

Stable ordered structures of Sn on Pt(111) (maximum coverage of 0.33 monolayers) were used as model catalysts to test the effect of tin and potassium on the hydrogenation of ethylene at 300 K and dehydrogenation of cyclohexane at 573 K and at pressures of 15 Torr of hydrocarbon and 100 Torr of H_2. Co-adsorption of tin and potassium on Pt(111) resulted in the direct interaction between potassium, tin, and platinum as verified by temperature-programmed desorption of CO. Tin deposition yielded a maximum in the turnover rate as a function of Sn coverage for ethylene hydrogenation and cyclohexane dehydrogenation with maxima at about 0.2 monolayers of tin and a turnover rate 75% higher than on clean Pt(111). This enhancement was explained by a lower rate of deactivation as tin was added. In contrast, the addition of potassium to Pt and Pt/Sn produced only a monotonic decrease in cyclohexane dehydrogenation. In an industrial system, where a higher tin coverage is used, interaction of tin with potassium may form an effective site blocker which could lower deactivation rates.

Key Words: **Pt(111); CO TPD on Pt(111)/Sn/K; hydrogenation of ethylene on Pt(111)/Sn/K; dehydrogenation of cyclohexane on Pt(111)/Sn/K.**

1. INTRODUCTION

Catalytic dehydrogenation processes are of increasing importance because of a growing demand for olefins such as propylene and isobutene. Isobutene is in particularly high demand as a feedstock for the production of oxygenated hydrocarbons required in reformulated gasoline, such as methyl-*tert*-butyl ether (MTBE), ethyl-*tert*-butyl-ether (ETBE), and *tert*-butyl alcohol (TBA). Supported platinum and platinum alloyed with other metals have long been used as dehydrogenation catalysts in catalytic reforming and in the production of olefins. For the latter application, the challenge has been how to produce a catalyst that will be stable and selective at the high temperature and low hydrogen partial pressure required to shift the equilibrium from the hydrocarbon toward the olefin. Thus, catalytic systems which can increase dehydrogenation selectivity and reduce coke formation at high temperature are highly desirable. Catalyst systems that employ Pt/Sn on a neutral support have been reported to exhibit high dehydrogenation selectivity and catalyst stability for dehydrogenation of light paraffins at elevated temperatures (1–3). In addition to the role of Sn, the dehydrogenation selectivity and deactivation stability are increased by the addition of potassium to a bimetallic Sn/Pt/silica catalyst (4, 5). In particular, Cortright and Dumesic (5) have reported that a $1:1:2.7$ $Pt/Sn/K/SiO_2$ catalyst could operate with minimum deactivation for many hours at 773 K with no H_2 added to the feed. These authors explained the synergistic effect of tin on the basis of a decrease in the size of surface Pt ensembles, suppressing hydrogenolysis and isomerization. Potassium (in the oxidized form) would also act as a blocking agent. Through microcalorimetric studies of ethylene, they also suggested that addition of Sn inhibits the formation of highly dehydrogenated surface species, leading to an increase in isobutene selectivity and a decrease in coke formation.

The objective of this work was to use ordered Sn structures, discovered by Paffet and Windham (6), as model catalysts to explore the effect of tin and potassium on hydrogenation and dehydrogenation reactions. These structures are obtained when Sn is deposited on Pt(111) forming a $p(2 \times 2)$ structure ($\Theta_{Sn} = 0.25$) and a $(\sqrt{3} \times \sqrt{3})R30^\circ$ structure ($\Theta_{Sn} = 0.33$). The advantage of this system is that it is ordered and thus the position of Sn is known. Its disadvantage is that the maximum Sn coverage is much lower than on systems of industrial importance.

The ordered structures of Sn on Pt(111) have been shown to inhibit the decomposition of ethylene (7), benzene (8), cyclohexene (9), and 1,3-cyclohexadiene (10) when these molecules were deposited on the surfaces and heated under ultrahigh vacuum. Catalytic studies on Sn/Pt(111) at

[1] Present address: Industrial Catalysis Research Team, Korea Research Institute of Chemical Technology, Jang-dong 100, Yusung-Gu, Taejon 305-606, Korea.

[2] Corresponding author. Current address: Worcester Polytechnic Institute, Department of Chemical Engineering, Worcester, MA 01609-2280. E-mail: fabio@wpi.edu.

0021-9517/98 $25.00

pressures close to one atmosphere have also been made (11–13). The effect of potassium on hydrocarbon adsorption and reaction on Pt(111) (14–16) as well as the effect of cesium (17, 18) have also been studied. However, no study is available for the influence of both tin and potassium on Pt(111) for hydrogenation and dehydrogenation catalytic reactions. For this reason, we studied a series of catalysts for the hydrogenation of ethylene and dehydrogenation of cyclohexane: Pt(111), K/Pt(111), Sn/Pt(111), and K/Sn/Pt(111). Although the Sn coverage on these model systems can reach a maximum Sn coverage of 0.33 monolayers and some of the reported catalysts in the literature have higher nominal tin coverage, we expected to verify a trend for the beneficial effect of Sn and K on increasing rates and decreasing deactivation for dehydrogenation reactions on these model catalysts. As a consequence, the results here should not be expected to reproduce the performance of industrial systems but to show the expected trend. We found that the effect of Sn seems to be one of decreasing the initial carbon buildup on the catalysts and potassium seems to act only as a site blocker. This role of potassium seems to be in conjunction with tin as we found that Sn–K–Pt forms a "surface alloy." Due to the large size of the potassium ion and its anchoring interaction with Sn, Sn–K may act in a similar way to Re–S on the Pt–Re–S system used in reforming as an effective site blocker. This last role has been proposed to decrease catalyst coking (19, 20) in reforming reactions. The addition of Sn and K does not make the catalyst more active it only makes it less prone to deactivation.

2. EXPERIMENTAL METHODS

Experiments were carried out in an ultra-high vacuum (UHV) chamber equipped with a high pressure reactor. After bakeout the chamber routinely attained a base pressure of 5×10^{-10} Torr (15). The analytical tools on the chamber are Auger electron spectroscopy (AES), low energy electron diffraction (LEED), mass spectrometry (UTI-100C) for temperature programmed desorption (TPD) as well as facilities for gas dosing and metal deposition. The high pressure batch reactor, which can be operated in the pressure range of 1 to 1000 Torr, is partly inside the UHV chamber. The reactor is engaged when the sample is enclosed by a hydraulically operated moving tube that seals the gases by means of a knife edged flange on a copper gasket (21). The reactor volume was 650 cm^3.

The Pt(111) was about 1 mm thick and about 1 cm^2, and was cut from bulk material (single crystal rods, Goodfellow) with 0.5° precision and polished with standard techniques (only one side was polished). The Pt(111) crystal mounting was accomplished via Pt heating wires spot welded to the crystal edge, enabling the surface to be resistively heated to 1200 K at a heating rate of up to 15 K s^{-1}. Temperature measurements were made using a chromel–alumel (type K) thermocouple spot welded to the rear side of crystal. The surface was cleaned in a vacuum by repeated cycles of Ar^+ sputtering, followed by oxidation at 800 K and subsequent annealing at 1073 K until no impurities could be detected by AES and a sharp (1×1) Pt(111) LEED pattern was observed.

Carbon monoxide TPD was carried in a line-of-sight mode with the mass spectrometer equipped with a cone-shaped nozzle that moved to 2 mm from the surface of the crystal. Carbon monoxide gas (Matheson, Research Grade) was dosed onto the crystal through a leak valve. During TPD experiments an Eurotherm controller model 818 with a TCR programmable DC supply from Electric Measurements, Inc. was used to ramp the temperature at a rate of 15 K s^{-1}.

Bimetallic surfaces were prepared by depositing tin on Pt(111) in UHV with a pulsed metal vapor vacuum arc plasma gun (MEVVA). The MEVVA source has been described in detail elsewhere (22, 23). Tin was deposited onto Pt(111) at room temperature, followed by annealing to 1000 K. The amount of adsorbed tin was controlled by varying the number of pulses from the evaporation source. Tin coverage was calibrated through AES and CO TPD.

Potassium deposition was achieved through a deposition system composed of a SAES getter source and a beam flag. The source was heated with a 5.4 amperes current and a different coverage could be achieved by varying the exposure time. The sample was kept at room temperature during deposition, followed by annealing to 600 K.

Hereafter all reported tin and potassium coverage will be expressed in monolayers (ML), defined as the atomic ratio of potassium or tin to the initial number of Pt surface atoms.

After tin and/or potassium deposition and associated surface compositional analysis the crystal was introduced into the high pressure reaction cell for hydrogenation/dehydrogenation reactions. A typical reaction was carried out as follows: (1) Ethylene hydrogenation; after introduction of ethylene (20 Torr), hydrogen (100 Torr), and helium (640 Torr) at room temperature the circulation pump was started to ensure the mixing of the reactant gases. (2) Cyclohexane dehydrogenation; after introduction of cyclohexane (15 Torr) and hydrogen (100 Torr) at room temperature the circulation pump was activated for a sufficient amount of time period to ensure the mixing of the reactant gases, followed by sample heating to 573 K. The reaction products were analyzed by direct injection through a gas valve into a gas chromatograph (Hewlett-Packard GC model 5720A and integrator model 3392) equipped with a flame ionization detector. After each reaction the reactor cell was pumped down with a diffusion pump before the cell was opened to the UHV chamber for postreaction surface analysis.

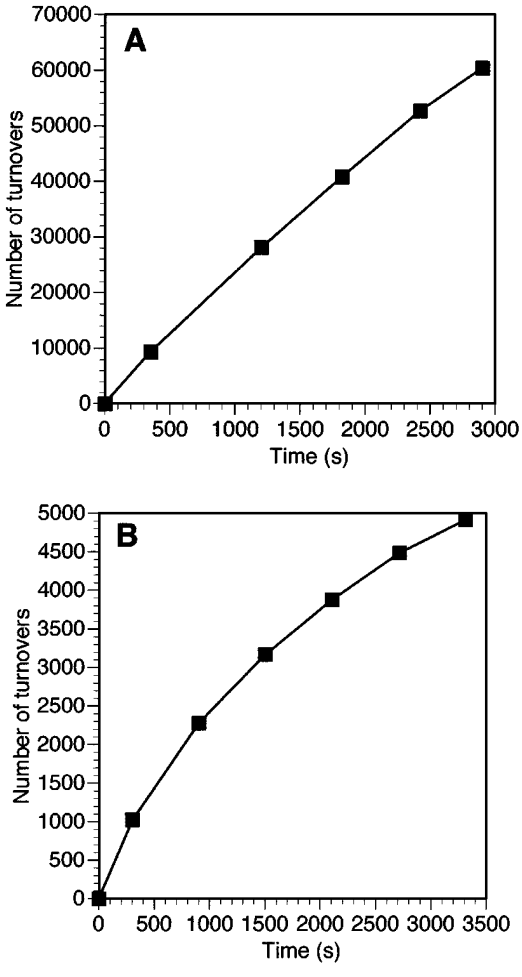

FIG. 1. Accumulation plots on Pt(111): (A) hydrogenation of ethylene at 20 Torr of ethylene, 100 Torr of H_2, 640 Torr of He, and reaction temperature of 302 K; (B) dehydrogenation of cyclohexane on Pt at 15 Torr of cyclohexane, 100 Torr of H_2, and reaction temperature of 573 K.

Research purity gases (Matheson) ethylene, isobutane, and hydrogen were used without further purification. Cyclohexane (Fluka, puriss) was used following several freeze-pump-thaw cycles for purification. Turnover rate (TOR) is the number of molecules produced per surface Pt atoms per second. The number of Pt atoms are the ones measured before reaction. The TOR reported in the results section represent reaction rates obtained after 30 min of reaction time. Typical accumulation plots for the ethylene and cyclohexane reactions are shown in Fig. 1.

3. RESULTS AND DISCUSSION

3.1. Characterization of K/Sn/Pt(111)

3.1.1. Calibration of Surface Composition of Sn and K on Pt(111) by AES, LEED, and CO TPD

The amount of tin deposited on Pt(111) was calibrated by AES measurements and by the ordered structures formed, as verified by LEED. The relationship between tin AES signal and exposure, expressed in terms of the number of pulses from the plasma source, was obtained using the AES uptake curves of both tin and platinum. The deflection points in Sn(430 eV) and Pt(64 eV) AES signals corresponding to successive monolayers could be seen clearly as the coverage evolved indicating layer-by-layer growth. After three equivalent monolayers, the Sn AES peak intensity was constant and it was not possible to use AES to monitor further Sn adsorption. When the crystal was annealed at 1000 K following tin deposition in excess of 0.5 ML (i.e., after 5 pulses of Sn) most of the tin dissolved into the bulk or evaporated leaving a constant tin coverage on the surface equivalent to 0.33 ML of surface atoms (Fig. 2). At this coverage a $(\sqrt{3} \times \sqrt{3})$R30° LEED structure was formed corresponding to a Pt_2Sn surface alloy (6). Upon annealing to 1000 K with an initial Sn coverage of less than 0.33 ML, the LEED pattern gradually changed from a p(1 × 1) to the more dense p(2 × 2) and finally to the $(\sqrt{3} \times \sqrt{3})$R30° structure. Even if excess tin was deposited, the $(\sqrt{3} \times \sqrt{3})$R30° LEED structure was always recovered following annealing to 1000 K. These results agree with these obtained by Paffett and Windham (6).

The potassium coverage on Pt(111) was also calibrated using AES uptake curves analogous to those employed for the Sn/Pt(111) system. Potassium deposition was controlled by varying the exposure time from the evaporating source. The potassium coverage was obtained using the uptake curve shown in Fig. 3, which clearly shows the deflection point corresponding to a single monolayer coverage. However, as the surface coverage increased above a monolayer successive deflection points could not be distinguished.

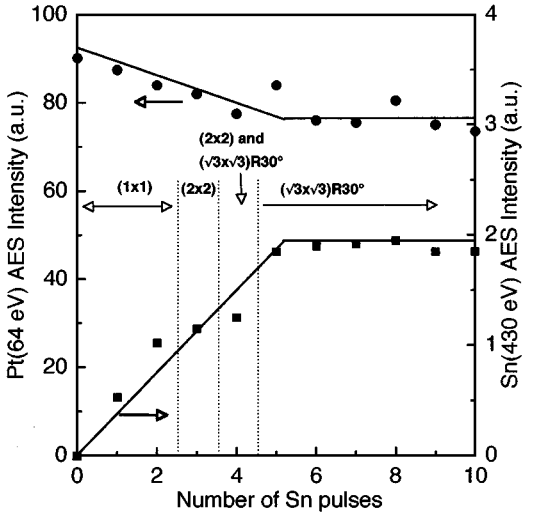

FIG. 2. Tin Auger uptake curves on Pt(111) surface. Sn(430 eV) and Pt(64 eV) peak intensities versus the number of Sn pulses with annealing at 1000 K after Sn deposition at 298 K. Ordered structures, as observed by LEED, are also shown.

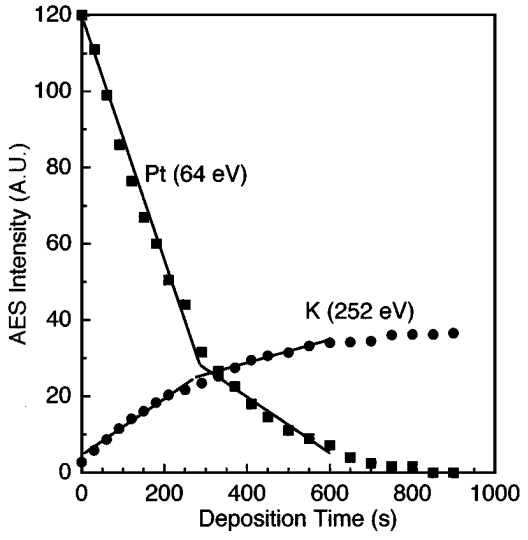

FIG. 3. Potassium Auger uptake curves on Pt(111) surface. K(252 eV) and Pt(64 eV) peak intensities versus exposing time with the crystal held at 298 K.

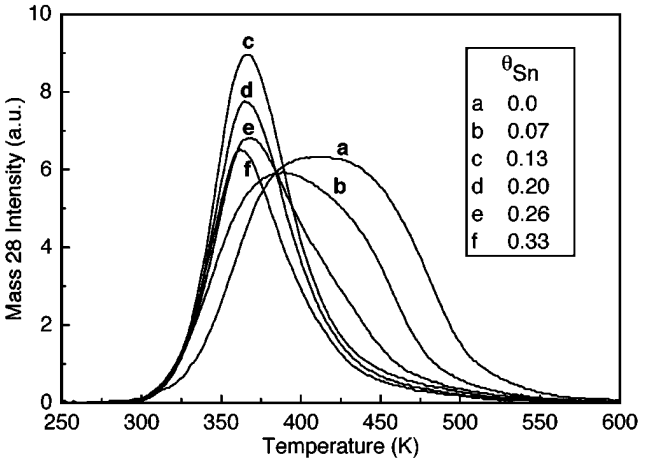

FIG. 4. Saturation CO TPD spectra from Sn/Pt(111) surface following annealing at 1000 K after Sn deposition at 298 K. The coverage was calibrated from Auger signal intensities. CO exposure at 1×10^{-7} Torr, 250 K for 5 min. The heating rate was 15 K s^{-1}.

The CO TPD results for Sn/Pt(111), K/Pt(111), and K/Sn/Pt(111) are discussed in turn. In general, the bonding of CO to metal atoms involves a synergistic electron transfer from the highest occupied molecular orbitals of CO (5σ) to the metal and, in turn, metal electrons are backdonated into the lowest unoccupied molecular orbital ($2\pi^*$) of CO (24, 25). Therefore, the presence of other metals on the Pt surface may change the bonding characteristic of CO. Any ad-atom which withdraws electrons from Pt will cause a decrease in the backdonation of metal electrons into the $2\pi^*$ CO and consequently weaken the metal–carbon bond while electron donation into Pt will produce the opposite effect. This effect will manifest itself as a change in the CO binding energy reflected in its desorption profile. It should be noted that other molecules (like hydrocarbons) may not interact with the surface in the same manner as CO and thus the TPD results obtained for CO cannot be extrapolated readily for other systems. There may also be other factors involved in displacing the CO desorption peak like the blocking of the preferred CO adsorption sites by another adsorbant (e.g., Sn and K) or the titration of defects on the crystal surface by Sn.

Figure 4 shows a series of saturation CO TPD spectra on Sn/Pt(111). The desorption peak is quite broad for a first-order desorption on Pt(111) but its shape changes as tin is added. For $\theta_{Sn} < 0.33$ the shift of the CO desorption peak to lower temperatures (425 to 365 K) with increasing tin coverage can indicate that on Pt(111) adsorbed Sn reduces the Pt–CO bond strength because of a Pt–Sn interaction, or that CO cannot bind on the same way because of geometric constraints (its preferred adsorption sites are now occupied by tin), or that there were defects on the crystal that were titrated by tin. This last possibility is discussed next. If it is assumed that the stoichiometry of CO to Pt is 2 to 1 on Pt(111) and that on defects (steps) the stoichiometry of CO to Pt is 1 to 1 as discussed before (26), then curve "c" in Fig. 4 predicts that at a coverage of tin of about 0.13 monolayers (adequate to cover all the defect sites) the ratio of CO areas for curves "a" and "c" should be as indeed observed in Fig. 5. The problem with this interpretation is that a much higher desorption temperature peak is expected for the step defects (about 550 K) and that about 15% of the Pt(111) surface atoms should be at step sites. Paffett *et al.* (27) studied the adsorption of CO on the Sn/Pt(111) structures and found the same broad peak for CO TPD and the same peak narrowing when Sn is added. They could rule out, however, by HREELS the possibility that the peak

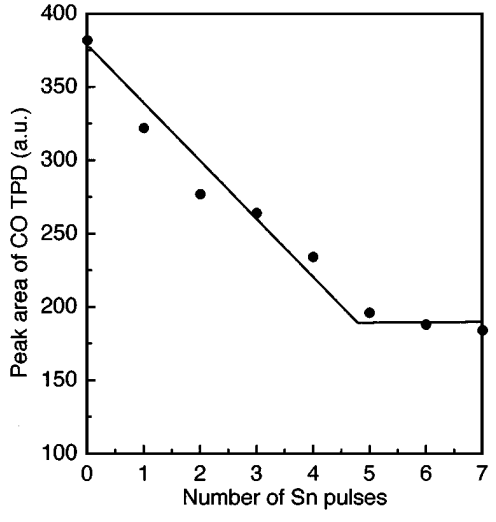

FIG. 5. Peak area of CO TPD versus Sn coverage. The area was obtained by integrating the CO TPD spectra of Fig. 4.

narrowing is caused by different CO chemisorption modes or by significantly different ratios of bridge versus atop adsorption. The peak narrowing may be a combination of different sites (less bridging sites available) and the titration of surface defects.

In the case of adsorbed Sn, the CO TPD exhibited a linear decrease in the peak area up to $\theta_{Sn} = 0.33$, indicating that CO adsorption does not occur on surface tin atoms (Fig. 5). For all Sn exposures corresponding to greater than five Sn pulses from the plasma source, Fig. 5 shows that the CO desorption peak area remains unchanged, indicating that a constant amount of tin always remains on the Pt(111) surface after annealing to 1000 K. The CO TPD results indicate a Sn coverage of 0.5 ML while the AES/LEED results suggest 0.33 ML coverage; tin seems to be blocking more than one CO site per Sn atom on the surface. Note that Paffet *et al.* (27) found that the number of Pt atoms counted by CO TPD blocking was higher than predicted on a Pt(111)/Sn surface while Haner *et al.* (28) found that CO could count perfectly the number of Pt atoms on the surface for single crystals made of Pt–Sn alloys. This discrepancy can be resolved if it is assumed that there are defects on the surface which adsorb with different stoichiometry. In view of the variation of counting Pt sites by CO TPD, we will use the AES results helped by LEED for the calculation of the amount of Pt on the surface. These values calculated from AES data are adequate for the purpose of this work.

Compared to tin, potassium on Pt(111) produced a bimodal CO desorption profile with a peak centered at approximately 425 and 640 K (Fig. 6), in contrast to a single peak at 425 K on the clean surface. This 215 K increase in desorption temperature, evident in the higher desorption peak, is a result of the electron donating ability of potassium, strengthening the Pt–CO bond. These two peaks reveal two environments for the CO: pure Pt and Pt modified

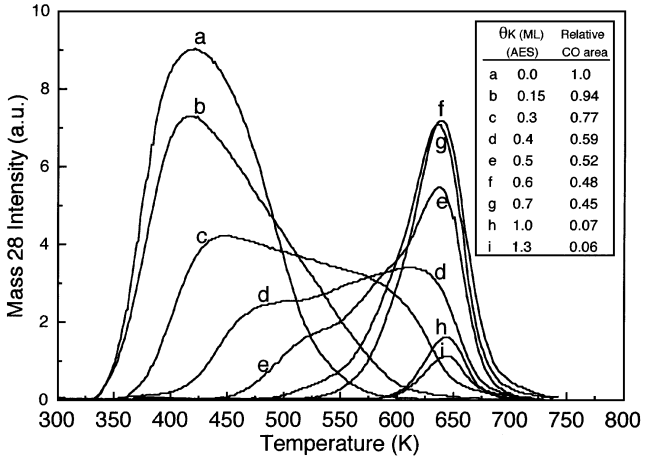

FIG. 6. Saturation CO TPD spectra from K/Pt(111) as a function of K coverage. The coverage was calibrated from Auger signal intensities. CO exposure at 1×10^{-7} Torr, 250 K for 5 min. The heating rate was 15 K s^{-1}.

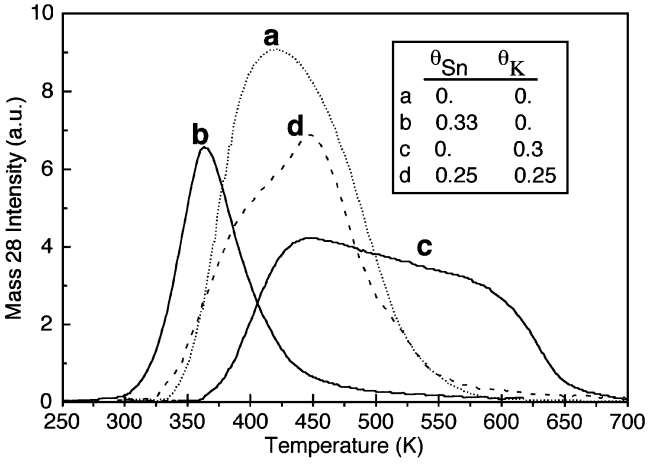

FIG. 7. Saturation CO TPD spectra from Sn/K/Pt(111). CO exposure at 1×10^{-7} Torr, 250 K for 5 min. The heating rate was 15 K s^{-1}.

by the potassium. As the potassium coverage increased, the desorption peak area at 640 K increased and that at 425 K decreased gradually. However, above one monolayer coverage ($\theta_K > 1.0$), almost all of the surface is potassium covered, as evidenced by the AES results, and consequently, no CO adsorption sites remain. This result can be interpreted on the basis that only exposed surface Pt atoms adsorb CO molecules while co-adsorbed potassium acts as an effective site blocker for CO adsorption. This is reflected in the monotonic decrease in CO TPD peak area with increasing K coverage (Fig. 6), indicating that, similar to the effect of Sn, CO does not adsorb on K. The apparent increase in CO binding energy induced by K co-adsorption is also consistent with results obtained by Crowell *et al.* (14) who found that the adsorption energy of CO is increased from 25 to 36 kcal mol^{-1} on potassium adsorbed Pt(111).

Having considered the independent interaction of Sn and K with Pt(111), the interaction of co-adsorbed tin and potassium with Pt(111) was studied next. The above CO TPD results over Sn/Pt(111) and K/Pt(111) systems reveal that the modification induced by tin and potassium have opposite trends on the Pt(111) surface. As shown in Fig. 7, when they are co-adsorbed on Pt(111), the TPD profile resembles that of CO adsorbed on clean Pt(111). This result implies that the effect of tin is compensated for by the effect of potassium. The other possibility is that the interaction of tin and potassium with platinum are independent of one another. However, this scenario would have yielded three different environments such as Pt, K/Pt, and Sn/Pt with three distinct CO desorption peaks at 425, 365, and 640 K, respectively. This is clearly in contrast to what is observed experimentally in Fig. 7, where curve "d" is not composed of curve "b" plus curve "c." Thus, *tin and potassium on Pt(111) form a three-component surface alloy*. A similar possibility was also raised by Spiewak *et al.* (29) to explain their results on $Pt/Sn/K/SiO_2$ catalysts but note that on their case the

potassium was present in the form of an oxide. These authors believe that the oxidized alkali interacts with tin forming a strong bond that anchors the alkali and provides further blocking.

In conclusion, the important facts from the CO TPD results are that there seems to be a compound formation on the surface by the interaction of tin, potassium, and platinum and that the effect of Sn on Pt seems to be one of titrating high energy sites. The other effects seems to be specific to CO because of the characteristic electronic structure of this molecule and they may be different for other probe molecules like hydrocarbons. The relationship between these surface modifications and hydrogenation and dehydrogenation are discussed in the next section.

3.2. Hydrogenation and Dehydrogenation Reactions

3.2.1. Ethylene Hydrogenation

Ethylene hydrogenation was carried out on tin covered Pt(111) after two different sample pretreatments and the results are shown in Fig. 8. The result for the Pt(111) with no Sn is a factor of about 4 higher than observed previously by Zaera and Somorjai (30) or reported in the literature (31). The reason for the higher rates is not known, although the most recent rates on Pt(111) and Pt foil reported on our group (32) were identical to the ones reported here. When the sample was annealed at 1000 K after tin deposition, the ethylene TOR showed a maximum at $\theta_{Sn} = 0.1$, corresponding to a 75% activity enhancement over clean Pt(111). In contrast, when the sample was not annealed following tin deposition, the activity enhancement was significantly less pronounced than that of the annealed sample (only 35% activity enhancement at $\theta_{Sn} = 0.07$). For these experiments, the annealing to 1000 K leads to a more homogeneous dispersion of tin on Pt(111) surface which seems to be necessary to attain the maximum increase in the rate for ethylene hydrogenation.

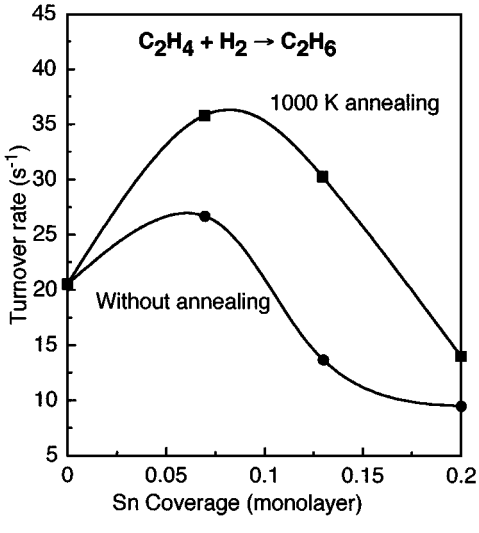

FIG. 8. Turnover rate for ethane production as a function of Sn coverage on Pt(111). Reaction condition; ethylene = 20 Torr, H_2 = 100 Torr, He = 640 Torr, and reaction temperature = 302 K. The turnover rate is based on the number of Pt atoms on the surface before reaction.

Windham *et al.* (16), Salmeron and Somorjai (33), and Berlowitz *et al.* (34) have shown for the saturation coverage of ethylene adsorbed on Pt(111) at 120 K that 60% of it desorbs molecularly upon heating, a small fraction (<2%) of ethane is produced, while the remainder of the adsorbed molecules decompose to produce a graphitic carbon residue and H_2 (g) during heating to 800 K. At a low ethylene coverage, all of the ethylene molecules adsorbed on clean Pt(111) decompose and desorption is completely irreversible. However, in the presence of Sn the ethylene adsorption strength is reduced, and no dissociation of ethylene occurs upon heating on the two Sn/Pt surface alloys having the p(2 × 2) and $(\sqrt{3} \times \sqrt{3})$R30° structures (7). The same is true for other molecules like benzene (8), cyclohexene (9), and 1,3-cyclohexadiene (10). Also, the activation energy decreases with the Sn surface concentration. Specifically, the activation energy of ethylene desorption was found to be 17 kcal mol^{-1} on Pt(111), falling to 15.1 and 11.8 kcal mol^{-1} on the p(2 × 2) alloy and $(\sqrt{3} \times \sqrt{3})$ alloys, respectively (7).

The lowering of the activation energy on the Sn/Pt surface could be due to a lower binding energy on Pt. Alternatively, different adsorption sites may exist for ethylene adsorbed on Pt in the p(2 × 2) and $(\sqrt{3} \times \sqrt{3})$ surfaces which have different heats of adsorption, although the properties of platinum itself has not been substantially modified by the addition of Sn. The existence of a different binding energy is supported by a previous study of C_2H_4/Bi/Pt(111), where the heat of ethylene adsorption on Bi/Pt(111) was found to be the same as ethylene on Pt(111) (35). Since Bi has a relatively small effect on the electronic structure of Pt and functions as a pure site blocking adatom on the Pt(111) surface (35), any change in the heat of ethylene adsorption on the Sn/Pt alloys is most likely due to a modification of surface Pt atoms, i.e. due to a ligand effect. This idea is also supported in the present study by the observation that a small amount of tin ($\theta_{Sn} = 0.1$), when alloyed with platinum, shifted CO desorption peak to lower temperature (Fig. 4). Note, however, that at the maximum ethylene TOR ($\theta_{Sn} = 0.1$), there is no observed structural changes in the LEED patterns from the clean p(1 × 1) Pt(111). The other interpretation is that the effect of tin could be to titrate the small amount of defects on the Pt surface. These defects are the source of carbonaceous deposits and, if not titrated before reaction, can decrease the overall rate by carbon deposition. Because we cannot account for a rate decrease due to carbon deposits (it is not measured; the amount of Pt exposed before reaction is used as a base to calculate turnover rates), a catalyst quickly poisoned by a higher

deposition rate of carbon would appear to have a lower rate and this is the reason why the rates appear to increase when tin is added. If tin were changing the binding energy and thus accelerating the rates, a monotonic increase of rate should be expected. Instead, the turnover rates actually decrease as more tin is added. Note that Paffett *et al.* (7) have shown that the adsorption sites suitable for reversible ethylene adsorption are more favorable on Sn/Pt(111) than on Pt(111). Again, the milder Sn/Pt surface does not form the carbonaceous precursors and appears as a catalyst with a higher rate, because under reaction conditions it has more Pt atoms exposed.

The effect of potassium on ethylene hydrogenation was not tested.

3.2.2. Cyclohexane Dehydrogenation

In dehydrogenation and hydrogenolysis reactions of cyclohexane over Pt crystals (36) the relative rate of dehydrogenation is several orders of magnitude higher than hydrogenolysis and isomerization, which results in only one dehydrogenation product (that is, benzene). Because of this specificity the reaction represents an ideal system to investigate dehydrogenation effects of tin and potassium on Pt(111). Cyclohexane dehydrogenation was carried out at 15 Torr cyclohexane, 100 Torr H_2 at 573 K with varied coverage of tin and potassium.

3.2.2.1. Sn/Pt(111). Figure 9 shows the effect of coadsorbed Sn on cyclohexane dehydrogenation. This figure shows a trend similar to that observed in ethylene hydrogenation (maximum activity at $\theta_{Sn} = 0.1$), where the catalyst exhibited maximum dehydrogenation activity at relatively low surface concentrations of tin ($\theta_{Sn} = 0.2$). At this point a 70% enhancement in activity was measured, compared to the clean Pt(111) (Fig. 9). The literature value for the turnover rate on Pt(111) extrapolated to our conditions is 14 s^{-1} (36). However, this value was measured at a lower temperature (533 K) and, due to severe deactivation at the higher temperature used in this work, a lower value for the turnover rate is expected.

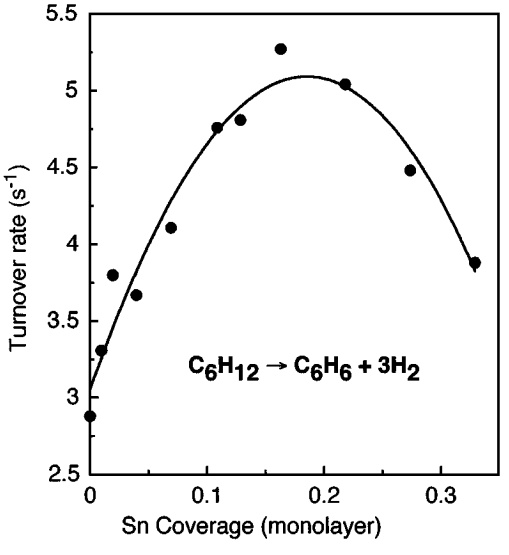

FIG. 9. Turnover rate for benzene production as a function of Sn coverage on Pt(111). The turnover rate is based on the number of Pt atoms on the surface before reaction. Reaction condition; cyclohexane = 15 Torr, H_2 = 100 Torr, and reaction temperature = 573 K.

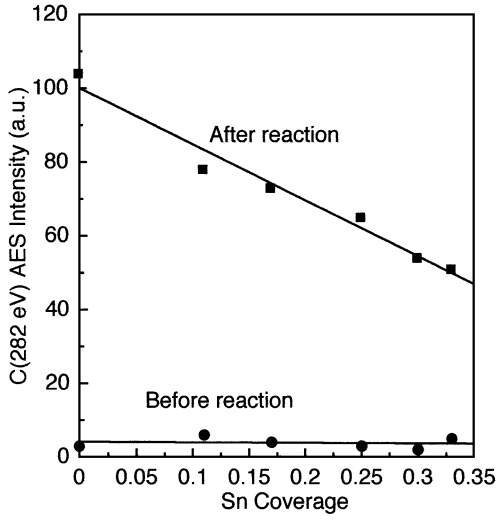

FIG. 10. Amount of carbon on the surface as a function of Sn coverage on Pt(111) after reaction with cyclohexane for about 1 h. Reaction condition; cyclohexane = 15 Torr, H_2 = 100 Torr, and reaction temperature = 573 K.

The Sn/Pt(111) system clearly showed a synergistic effect in both hydrogenation and dehydrogenation reactions. It is clear that on Pt(111) a higher final rate for hydrogenation and dehydrogenation activity is obtained when tin is added at about 0.2 monolayers. To check the dependence of catalyst structure for the cyclohexane dehydrogenation, reactions were carried out over p(2 × 2) and $(\sqrt{3} \times \sqrt{3})$R30° Sn/Pt(111) alloys. The Sn/Pt(111) having these structures did not show any special enhancement in activity, compared to the primitive (1 × 1); in fact the turnover rate was lower on these structures. The higher turnover rate enhancement appeared at $\theta_{Sn} = 0.2$, where there are no extra structures on the surface except the p(1 × 1) structure. As already advanced in the earlier section, this volcano curve could be due to a lower rate of deactivation on the catalysts that occurs by the titration of platinum sites by tin or by a less reactive platinum surface obtained by the addition of tin. If this argument is valid, then the amount of carbon deposited should decrease as tin is added to the surface as indeed shown in Fig. 10.

The fact that the rates decreased after the maximum and did not stay constant as expected for a structure-insensitive reaction cannot be explained easily. Cortright and Dumesic (5) also found that the turnover rates for the dehydrogenation of isobutane decreased by the addition of Sn. This

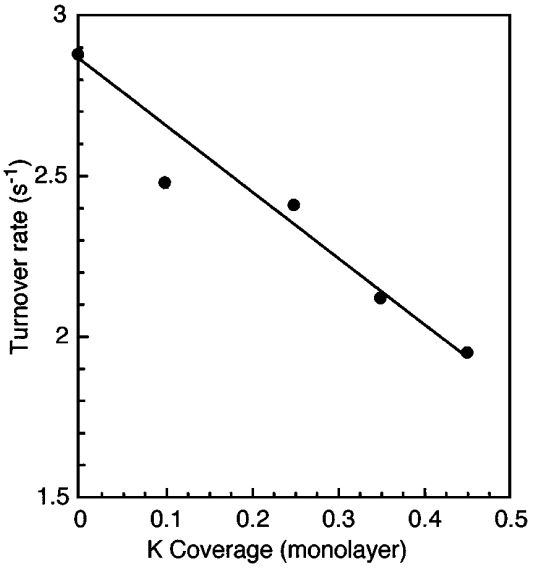

FIG. 11. Turnover rate for benzene production as a function of K coverage on Pt(111). Reaction condition; cyclohexane = 15 Torr, H_2 = 100 Torr, and reaction temperature = 573 K. The turnover rate is based on the number of Pt atoms on the surface before reaction.

volcano-type plot was also found by Szanyi *et al.* (11) for the reaction of *n*-butane hydrogenolysis. These authors found that the TOR for the p(2 × 2) structure was higher than for Pt(111) but then decreased again as more Sn was added to form the $(\sqrt{3}\times\sqrt{3})$R30° structure. A change in the binding energy of reaction intermediates that will in turn affect the turnover rate would be a possible explanation.

3.2.2.2. K/Pt(111). Figure 11 shows that the TOR decreased linearly with potassium coverage. This linear decrease in activity over the whole coverage range implies that the electron donation associated with potassium adsorption on metals does not affect the dehydrogenation of cyclohexane. Potassium itself is inactive in cyclohexane dehydrogenation and, as a result, at monolayer coverage K/Pt(111) showed almost no activity.

Based on the results of Zaera and Somorjai (15), the interaction of *n*-hexane on K/Pt(111) is characterized by a decrease in the sticking coefficient of *n*-hexane. In this process, at least one C–H bond-breaking event takes place, followed by the formation of a carbon–metal bond between the metal and alkyl fragment. This adsorption is accompanied by charge transfer from the hydrocarbon to the platinum, leaving the former with a carbonium ion character. Potassium on the surface, acting as an electron donor, inhibits this charge transfer, making the C–H bond-breaking process less favorable. Accordingly, this effect should be more accentuated as the alkyl fragment continues to dehydrogenate, Zaera and Somorjai have showed that the presence of potassium on Pt(111) produced a steep rise in the activation energy for hydrogen β elimination of the carbonaceous deposits. Based on these results, the fact that the turnover rate decreases with the amount of potassium on the surface (note that the turnover rate is already corrected for blocking effects), the presence of potassium makes C–H bond-breaking more difficult and reduces the dehydrogenation activity. Again, the addition of potassium seems to make it difficult to form highly dehydrogenated species that may deactivate the catalyst.

3.2.2.3. K/Sn/Pt(111). Additional dehydrogenation experiments were carried out on the four catalyst series, Pt(111), Sn/Pt(111), K/Pt(111), and K/Sn/Pt(111). The turnover rate for these four catalysts are shown in Fig. 12. Among these four catalysts, Sn/Pt(111) showed the highest turnover rate. When potassium was added to Sn(0.25)/Pt(111), the activity gradually decreased in an analogous trend to the results observed for cyclohexane dehydrogenation over K/Pt(111) (Fig. 11). Thus, regardless of the presence or absence of tin, the addition of potassium causes the turnover rates to decrease, with no apparent advantage for the use of potassium on Sn/Pt catalysts.

However, in contrast to our observations, there are results reported in the literature to support the idea that the addition of potassium on Sn/Pt/supported catalysts increases both dehydrogenation turnover rate and catalytic stability (4, 5, 37–41). These results are actually in line with our findings as will be explained in turn. On supported catalysts the high surface area support may play a role in the kinetics and in our studies there is no support present. It is

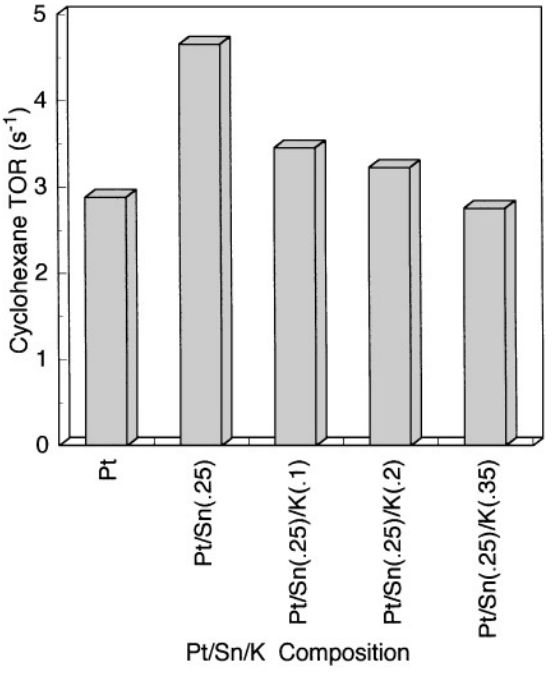

FIG. 12. Turnover rate for benzene production as a function of K and Sn coverage on Pt(111). Reaction condition; cyclohexane = 15 Torr, H_2 = 100 Torr, and reaction temperature = 573 K. The turnover rate is based on the number of Pt atoms on the surface before reaction.

well known that the presence of acidic supports can result in the catalysis of undesired parallel reactions (cracking and polymerization) and for this reason, an increasing number of papers have been published recently on the use of acidic supports suitably modified by alkali metals (37, 38) since the alkali will neutralize the acidity. However, it seems that at least the effect of potassium reported by Cortright and Dumesic (4, 5, 42) is not related to that cause. These authors found that in their supported catalyst system for isobutane dehydrogenation, potassium is important for the selectivity and stability of the catalyst. Our results suggest that potassium does not modify drastically the catalytic properties of Pt/Sn/K catalysts. It certainly does not increase the turnover rate but it may provide for additional or a better site blocker as suggested by Cortright and Dumesic (5). This is a plausible explanation for the effect of K since our CO TPD results suggest that the Sn and K are interacting and thus the Sn–K system would be similar to the Re–S moiety formed on the Pt–Re–S system, with K interacting with Sn and acting as an effective site blocker (like S in the Re–S system), making it difficult to form carbonaceous deposits. The reason we could not find the same enhancement for K and Sn as reported by Cortright and Dumesic may be related to the much higher Pt to Sn ratio in our studies. As explained before, we could not decrease the ratio below Pt/Sn = 3. The number of contiguous Pt sites for the $(\sqrt{3}\times\sqrt{3})R30^\circ$ structure is still very large for this catalyst to be significantly better than Pt on its deactivation pattern. In the same way, the blocking effect of K (by the K–Sn interaction) cannot be seen at this low dilution of Sn on Pt. The most resistant catalysts to deactivation reported in the literature are the ones with a low Pt/Sn ratio (Pt/Sn = 0.25). Thus, as in the case of Pt–Re–S, for the effect of K to be seen in creating a more stable catalyst the amount of Sn on the surface should be high (not attainable in our case) and we cannot make a direct comparison of our samples with the supported catalysts. For this reason, it is possible to observe an increase in turnover rate (actually a lower deactivation rate) when tin and potassium are added simultaneously at a high coverage as Cortright and Dumesic (5) have found.

The other difference in our studies was that the addition of Sn caused a volcano type curve, not reported for supported catalysts. The reason for that is due to the different defect densities and deactivation mechanism on the two systems. We can prepare pristine samples and preserve them before reaction. These samples have very high activity sites that will not be present on supported catalysts because these sites are highly reactive and during the normal supported catalyst preparation they will be poisoned before the reaction can start. These sites can, however, be poisoned by the addition of Sn on the model catalysts. We have seen before that the effect of Sn on a polycrystalline Pt foil was to titrate the highly active and coke forming centers before reaction (26). In the present case, Sn has the same role as before and the initial increase in activity is due to the titration of the highly active and coke-forming sites which poison the catalyst before kinetic measurements can be made. The addition of Sn will then imply a lower amount of carbon deposits as indeed observed (Fig. 10).

SUMMARY

The adsorption of tin on Pt(111) decreased the tendency of the surface to deactivate by carbon deposition (coking). This was verified directly by the decrease of carbon buildup after reaction with cyclohexane. These results point to Sn titrating the high activity, coke-forming defect sites present on Pt(111) or impeding the formation of highly unsaturated molecules by making the presence of large ensembles of Pt unavailable. This decrease in carbon buildup explains the increase in rates for hydrogenation of ethylene and dehydrogenation of cyclohexane when less than 0.2 monolayers of Sn is added.

In the presence of both tin and potassium the CO TPD suggests an interaction between K and Sn with the formation of a "surface alloy." Adsorbed potassium decreased the turnover rate of cyclohexane dehydrogenation on Pt and Pt/Sn samples with a monotonic decrease in activity with increasing potassium coverage. Potassium could possibly decrease the rate of deactivation by site blocking, especially because K has a large ionic radius, it interacts with Sn, and there is an example in the literature of a similar effect of bulky surface compounds like Re–S on the Pt–Re–S system increasing the catalyst stability.

The Pt/Sn/K catalyst is a better catalyst for dehydrogenation because it deactivates less, not because it has a higher turnover rate.

ACKNOWLEDGMENTS

This work was supported by the Director, Office of Energy Research, Office of Basic Energy Sciences, Materials Sciences Division, of the U.S. Department of Energy under Contract DE-AC03-76SF00098. Y.-K. Park thanks Dr. D. H. Fairbrother for his help.

REFERENCES

1. Miller, S. J., U.S. Patent 4,727,216 (1986).
2. Brinkmeyer, F. M., and Rohr, D. F., U.S. Patent 4,866,211 (1987).
3. Imai, T., and Hung, C. W., U.S. Patent 4,430,517 (1983).
4. Cortright, R. D., and Dumesic, J. A., *J. Catal.* **148**, 771 (1994).
5. Cortright, R. D., and Dumesic, J. A., *J. Catal.* **157**, 576 (1995).
6. Paffett, M. T., and Windham, R. G., *Surf. Sci.* **208**, 34 (1989).
7. Paffett, M. T., Gebhard, S. C., Windham, R. G., and Koel, B. E., *Surf. Sci.* **223**, 449 (1989).
8. Xu, C., Tsai, Y. L., and Koel, B. E., *J. Phys. Chem.* **98**, 585 (1994).
9. Xu, C., and Koel, B. E., *Surf. Sci.* **304**, 249 (1994).
10. Peck, J. W., and Koel, B. E., *J. Am. Chem. Soc.* **118**, 2708 (1996).
11. Szanyi, J., Anderson, S., and Paffett, M. T., *J. Catal.* **149**, 438 (1994).
12. Szanyi, J., and Paffett, M. T., *Catal. Lett.* **29**, 133 (1994).
13. Szanyi, J., and Paffett, M. T., *J. Am. Chem. Soc.* **117**, 1034 (1995).

14. Crowell, J. E., Garfunkel, E. L., and Somorjai, G. A., *Surf. Sci.* **121**, 303 (1982).
15. Zaera, F., and Somorjai, G. A., *J. Catal.* **84**, 375 (1983).
16. Windham, R. G., Bartram, M. E., and Koel, B. E., *J. Phys. Chem.* **92**, 2862 (1988).
17. Davidsen, J. M., Henn, F. C., Rowe, G. K., and Campbell, C. T., *J. Phys. Chem.* **95**, 6632 (1991).
18. Bussell, M. E., Henn, F. C., and Campbell, C. T., *J. Phys. Chem.* **96**, 5978 (1992).
19. Sachtler, W. M. H., *J. Mol. Catal.* **25**, 1 (1984).
20. Ribeiro, F. H., Bonivardi, A. L., Kim, C., and Somorjai, G. A., *J. Catal.* **150**, 186 (1994).
21. Kahn, O. R., Petersen, E. E., and Somorjai, G. A., *J. Catal.* **34**, 294 (1974).
22. Kim, C., Ogletree, D. F., Salmeron, M. B., Godechot, Y., Somorjai, G. A., and Brown, I. G., *Appl. Surf. Sci.* **59**, 261 (1992).
23. Kim, C., and Somorjai, G. A., *J. Catal.* **134**, 179 (1992).
24. Doyen, G., and Ertl, G., *Surf. Sci.* **43**, 197 (1974).
25. Nieuwenhuys, B. E., *Surf. Sci.* **105**, 505 (1981).
26. Fujikawa, T., Ribeiro, F. H., and Somorjai, G. A., *J. Catal.* **178**, 58 (1998).
27. Paffett, M. T., Gebhard, S. C., Windham, R. G., and Koel, B. E., *J. Phys. Chem.* **94**, 6831 (1990).
28. Haner, A. H., Ross, P. N., Bardi, U., and Atrei, A., *J. Vac. Sci. Technol. A* **10**, 2718 (1992).
29. Spiewak, B. E., Levin, P., Cortright, R. D., and Dumesic, J. A., *J. Phys. Chem.* **100**, 17260 (1996).
30. Zaera, F., and Somorjai, G. A., *J. Am. Chem. Soc.* **106**, 2288 (1984).
31. Ribeiro, F. H., Schach von Wittenau, A. E., Bartholomew, C. H., and Somorjai, G. A., *Catal. Rev. Sci. Eng.* **39**, 49 (1997).
32. Quinlan, M. A., Ph.D. thesis, University of California at Berkeley, 1996.
33. Salmeron, M., and Somorjai, G. A., *J. Phys. Chem.* **86**, 341 (1982).
34. Berlowitz, P., Megris, C., Butt, J. B., and Kung, H. H., *Langmuir* **1**, 206 (1985).
35. Windham, R. G., Koel, B. E., and Paffett, M. T., *Langmuir* **4**, 1113 (1988).
36. Herz, R. K., Gillespie, W. D., Petersen, E. E., and Somorjai, G. A., *J. Catal.* **67**, 371 (1981).
37. Gravelle-Rumeau-Maillot, M., Pitchon, V., Martin, G. A., and Praliaud, H., *Appl. Catal. A* **98**, 45 (1993).
38. de Miguel, S., Castro, A., Scelza, O., Fierro, J. L. G., and Soria, J., *Catal. Lett.* **36**, 201 (1996).
39. Park, Y., and Price, G. L., *Ind. Eng. Chem. Res.* **31**, 469 (1992).
40. Davis, R. J., and Derouane, E. G., *J. Catal.* **132**, 269 (1991).
41. Clarke, J. K. A., Bradley, M. I., Carvie, L. A. J., Craven, A. J., and Baird, T., *J. Catal.* **143**, 122 (1993).
42. Cortright, R. D., and Dumesic, J. A., *Appl. Catal. A* **129**, 101 (1995).